https://doi.org/10.5194/acp-2019-508
Preprint. Discussion started: 14 June 2019

Atmospheric Chemistry and Physics Discussions

On the impact of future climate change on tropopause folds and tropospheric ozone

Dimitris Akritidis[1], Andrea Pozzer[2], and Prodromos Zanis[1]

[1]Department of Meteorology and Climatology, School of Geology, Aristotle University of Thessaloniki, Thessaloniki, Greece
[2]Max Planck Institute for Chemistry, Mainz, Germany

Correspondence: D. Akritidis (dakritid@geo.auth.gr)

Abstract. Using a transient simulation for the period 1960-2100 with the state-of-the-art ECHAM5/MESSy Atmospheric Chemistry (EMAC) global model and a tropopause fold identification algorithm, we explore the future projected changes in tropopause folds, Stratosphere-to-Troposphere Transport (STT) of ozone and tropospheric ozone under the RCP6.0 scenario. Statistically significant changes in tropopause fold frequencies are identified in both Hemispheres, occasionally exceeding 3%, which are associated with the projected changes in the position and intensity of the subtropical jet streams. A strengthening of ozone STT is projected for future at both Hemispheres, with an induced increase of transported stratospheric ozone tracer throughout the whole troposphere, reaching up to 10 $\mathrm{nmol/mol}$ in the upper troposphere, 8 $\mathrm{nmol/mol}$ in the middle troposphere and 3 nmol/mol near the surface. Notably, the regions exhibiting the maxima changes of ozone STT at 400 hPa, coincide with that of the highest fold frequencies, highlighting the role of tropopause folding mechanism in STT process under a changing climate. For both the eastern Mediterranean and Middle East (EMME), and the Afghanistan (AFG) regions, which are known as hotspots of fold activity and ozone STT during the summer period, the year-to-year variability of middle tropospheric ozone with stratospheric origin is largely explained by the short-term variations of ozone at 150 hPa and tropopause folds frequency. Finally, ozone in the lower troposphere is projected to decrease under the RCP6.0 scenario during MAM (March, April and May) and JJA (June, July and August) at the Northern Hemisphere, and during DJF (December, January and February) at the Southern Hemisphere, due to the decline of ozone precursors emissions, while in the rest of the troposphere ozone shows a remarkable increase owing to the STT strengthening.

1 Introduction

Tropospheric ozone plays a key role in the oxidizing capacity of the atmosphere (Lelieveld et al., 2016), it is also a short-lived climate forcer being an important greenhouse gas, while near the surface it is a pollutant detrimental to human health, crops and ecosystems (Monks et al., 2015). The future tropospheric ozone changes in global scale depend on changes of the processes that control tropospheric ozone budget, namely, chemical ozone production and loss, Stratosphere-Troposphere Exchange (STE) and deposition (Young et al., 2013). The net stratospheric influx results from STE processes, comprised of Troposphere-to-Stratosphere Transport (TST) and Stratosphere-to-Troposphere Transport (STT) with tropopause folds considered as the main mechanism for stratospheric intrusions in STT events (Stohl et al., 2003). In the 21^{th} century, emissions of ozone precursor

https://doi.org/10.5194/acp-2019-508
Preprint. Discussion started: 14 June 2019

Atmospheric Chemistry and Physics Discussions

species, ozone depleting substances (ODSs) and long-lived greenhouse gases (GHGs) are expected to be the major factors governing ozone amounts and its distribution in the troposphere and the stratosphere (Fiore et al., 2015; Revell et al., 2015). More specifically, future changes of the net stratospheric influx in STE are linked to changes of the stratospheric Brewer-Dobson Circulation (BDC) and the amount of ozone in the lowermost stratosphere, which are strongly influenced in a changing climate by the emissions of ODSs and GHGs (Oberländer-Hayn et al., 2016; Morgenstern et al., 2018).

Predominantly, the foldings of the tropopause are of limited vertical extend and their global spatiotemporal distribution is mainly controlled by the location and intensity of the jet stream, as in principle, they are developed through ageostrophic flow in the proximity of the jet stream (Stohl et al., 2003). Deep folds extending down to the lower troposphere and occasionally to the ground surface may lead to irreversible mixing of stratospheric air into the troposphere, and thus, to chemical composition changes (Cristofanelli et al., 2006; Akritidis et al., 2010; Lin et al., 2015; Knowland et al., 2017). During the recent years, several modeling studies indicated that the stratospheric contribution to tropospheric and near-surface background ozone may be of greater importance than previously anticipated (Zhang et al., 2011; Lin et al., 2012; Zanis et al., 2014; Lefohn et al., 2014; Akritidis et al., 2016; Williams et al., 2019).

Changes in ozone precursor emissions have the largest effect on future tropospheric ozone concentrations. Future reductions in most ozone precursor emissions, which is a common feature across the Representative Concentration Pathways (RCPs), drive tropospheric ozone decreases, except for RCP8.5 that show an increase due to much larger methane concentrations compared to the other RCPs (Stevenson et al., 2006; Naik et al., 2013; Young et al., 2013; Sekiya and Sudo, 2014; Revell et al., 2015; Banerjee et al., 2016; Meul et al., 2018). Future decreases in ODS may lead to an ozone increase essentially everywhere in the atmosphere, with the largest percentage changes in the upper stratosphere and the lower stratosphere at high latitudes due to the anticipated ozone recovery, while changes in GHGs may lead to a decrease in the tropical lower stratosphere and an increase of STE due to strengthening of the BDC (Morgenstern et al., 2018). The 2014 Ozone Assessment (Carpenter et al., 2014) highlighted that Chemistry Climate Models (CCMs) robustly predict a long term acceleration of the BDC in response to anthropogenic climate change (Hardiman et al., 2014; Palmeiro et al., 2014) which also stands for the new CCMI (Chemistry-Climate Model Initiative) simulations (Morgenstern et al., 2018).

Several recent studies with CCMs provide evidence that both the acceleration of the BDC and stratospheric ozone recovery will tend to increase the future global tropospheric ozone burden through enhanced STE with the magnitude of the change depending on the RCP scenario, partially offsetting tropospheric ozone decreases associated with reductions in ozone precursor emissions (Sekiya and Sudo, 2014; Banerjee et al., 2016; Meul et al., 2018). Banerjee et al. (2016) showed that BDC strengthening under the RCP8.5 has the largest impact on tropospheric ozone over the tropics and subtropics, while stratospheric ozone recovery from declining ODSs becomes more important in the mid-latitudes and extratropics. Meul et al. (2018) simulated that the global mean annual STT is projected to increase by 53% between the years 2000 and 2100 under RCP8.5 and it will be smaller for RCP6.0, but the resulting relative change in the contribution of ozone with stratospheric origin to ozone in the troposphere is of comparable magnitude in both scenarios. The covariability between STE and tropospheric ozone from observations was used to deduce that the projected future strengthening of the BDC alone (without accounting for ozone recovery), could lead to an increase in zonal-mean tropospheric ozone of 2% by the end of the 21st century (Neu et al., 2014).

https://doi.org/10.5194/acp-2019-508
Preprint. Discussion started: 14 June 2019

Atmospheric Chemistry and Physics Discussions

Hess et al. (2015) extrapolating their model results from present time to future, concluded that a 30% increase in the ozone flux by 2100 due to BDC strengthening would result in a 3% increase in surface ozone and a 6% increase in mid-tropospheric ozone. However, Morgenstern et al. (2018) using simulations from multiple CCMs showed that the surface ozone response to anthropogenic forcings from well-mixed GHGS and ODS remains uncertain, reflecting uncertainties related to STE. It is therefore crucial to conduct more studies towards this direction, in order to increase confidence in the future projected changes of tropospheric ozone and its associated drivers.

This study aims to assess the impacts of future climate change under the RCP6.0 scenario on tropopause folds and tropospheric ozone, using a free-running hindcast and projection ECHAM5/MESSy (EMAC) simulation for the period 1960-2100. To this end, a 3-D labeling algorithm is implemented to detect tropopause folds in EMAC simulation. Besides ozone, a tracer for stratospheric ozone is also employed to investigate the projected changes in STE of ozone. Section 2 presents the main characteristics of the EMAC model and describes the 3-D labeling algorithm used to detect the folding events. Section 3 and 4 show the key results of the current study, and finally, Section 5 summarizes the main conclusions.

2 Methodology

2.1 EMAC model

The ECHAM5/MESSy Atmospheric Chemistry (EMAC) global model is a numerical chemistry and climate simulation system that includes sub-models describing tropospheric and middle atmosphere processes and their interactions with ocean, land and human activities (Jöckel et al., 2010). It uses the second version of the Modular Earth Submodel System (MESSy2) to link multi-institutional computer codes. The core atmospheric model is the 5^{th} generation circulation model (ECHAM5, Roeckner et al., 2006). The EMAC model has been extensively evaluated for gas tracers (e.g. Pozzer et al., 2007) and for aerosols (e.g. Pringle et al., 2010; Pozzer et al., 2012; Astitha et al., 2012). For the present study we use ECHAM5 version 5.3.02 and MESSy version 2.51. More specifically, data from the simulation RC2-base-04 are used, which is part of the set of simulations performed within the ESCiMo project (Jöckel et al., 2016). The model horizontal resolution is T42L90MA, i.e. with a spherical truncation of T42 (corresponding to a quadratic Gaussian grid of approx. 2.8 by 2.8 degrees in latitude and longitude) with 90 vertical hybrid pressure levels up to 0.01 hPa.

The simulation covers the time frame 1960-2100 (10 years spin-up from 1950 to 1959) driven by prescribed Sea Surface Temperature (SST) and Sea Ice Coverage (SIC) taken from simulations with the global climate model HadGEM2-ES (Collins et al., 2011; Martin et al., 2011) for the Coupled Model Intercomparison Project phase 5 (CMIP5). Anthropogenic emissions are incorporated as prescribed emission fluxes following the CCMI recommendations (Eyring et al., 2013). In more detail, the emissions data set consists of a combination of ACCMIP (Lamarque et al., 2010, for the 1950-2000 period) and RCP6.0 data (Fujino et al., 2006, for the 2000 and on). A detailed description of the simulation can be found in (Jöckel et al., 2016, and references therein).

Along with ozone chemistry, EMAC also includes a tracer for ozone of stratospheric origin, denoted by O3s, which provides an indicator of the stratospheric contribution to tropospheric ozone. In the stratosphere, O3s is equal to ozone values, while

https://doi.org/10.5194/acp-2019-508
Preprint. Discussion started: 14 June 2019


Atmospheric Chemistry and Physics Discussions

in the troposphere it follows the transport and destruction processes of ozone. When O3s returns to the stratosphere it is reset to stratospheric values; however, since it is initialized above 100 hPa, only a very small fraction is recirculated by multiple crossings of the tropopause (Roelofs and Lelieveld, 1997).

2.2 Tropopause fold identification

In this work the algorithm developed by Sprenger et al. (2003) and improved by Škerlak et al. (2015) has been adopted and applied in order to detect tropopause folds in EMAC simulation (as in Akritidis et al. (2016)), using the 3-D fields of potential vorticity, potential temperature and specific humidity. As in several previous studies (Hoskins et al., 1985; Holton et al., 1995; Stohl et al., 2003; Sprenger et al., 2003), the tropopause is defined as the combination of the isosurfaces of potential vorticity at ± 2 PVU and potential temperature at 380 K, whichever is lower (refered as dynamical tropopause). For each grid point a tropopause fold is designated where multiple crossings of the dynamical tropopause are detected in instantaneous vertical profiles. Subsequently, the upper (p_U), middle (p_M), and lower (p_L) pressure levels of tropopause crossings are determined and the pressure difference $\Delta p = p_M - p_U$ between the upper and middle tropopause crossings is calculated (for more details see Fig.1 Tyrlis et al. (2014)). The above pressure difference reveals the vertical extent of the tropopause fold, and is used to classify the identified folds into three categories (for more details see Škerlak et al., 2015):

- shallow folds, $50 \leq \Delta p < 200$ hPa
- medium folds, $200 \leq \Delta p < 350$ hPa
- deep folds, $\Delta p \geq 350$ hPa

Before the results from simulation RC2-base-04 can be used to estimate the future projected changes of fold frequencies, the capability to reproduce present-time folding frequencies must be first ckecked. Therefore the model results have been compared with the monthly fold frequencies climatology compiled by Škerlak et al. (2015). The climatology has been calculated using the same identification algorithm used in this work from the ERA-interim dataset (Dee et al., 2011). Figure 1 shows the mean hemispheric (0-65°N and 0-65°S) monthly frequencies of different folding categories calculated from the results of simulation RC2-base-04 for the period 1979-2012, the exact same one covered by the work of Škerlak et al. (2015). This figure can be compared with Figure 7 of the Škerlak et al. (2015) manuscript. The results are similar, implying a good representation of present-time monthly folding frequency. Additionally, not only the hemispheric monthly fold frequencies are similar between data from simulation RC2-base-04 and data from ERA-Interim, but also the geographical distribution presents the same patterns (not shown). We can therefore consider that the data used in this work are comparable for present-time with state-of-the-art calculations based on the ERA-Interim dataset.

3 Future projected changes

To explore the future projected changes in EMAC meteorological and chemical parameters under the RCP6.0 emissions scenario, we consider two 30-years time periods: a) present-day climate used as reference (REF) spanning from 1970 to 1999

https://doi.org/10.5194/acp-2019-508
Preprint. Discussion started: 14 June 2019

Atmospheric Chemistry and Physics Discussions

and b) future climate (FUT) spanning from 2070 to 2099. The selection of a 30-years period for the climate representation is complying with World Meteorological Organization's (WMO) suggestion (WMO, 2011). All seasons in the manuscript refer to boreal seasons (winter: DJF, spring: MAM, summer: JJA, autumn: SON).

3.1 Jet streams and tropopause folds

At first, the impact on atmospheric circulation under the RCP6.0 scenario is explored. As it is depicted from Figure 2 there is a distinct upward and poleward shift in the Southern Hemisphere (SH) midlatitude jet during all seasons, which is also identified during DJF and SON at the Northern Hemisphere (NH), yet less pronounced. A poleward-upward shift of the westerly jet in response to greenhouse warming, was reported by several previous studies using individual models (Butler et al., 2010; Orbe et al., 2015; Doherty et al., 2017) or ensembles of models participating in the Intergovernmental Panel on Climate Change (IPCC) 4^{th} assessment report (Lorenz and DeWeaver, 2007), and the Coupled Model Intercomparison Project phase 3 (CMIP3) and phase 5 (CMIP5) (Swart and Fyfe, 2012; Delcambre et al., 2013; Yim et al., 2016). Moreover, a rise of the tropopause is seen during all seasons at both the NH and SH extratropics, which in an annual basis is estimated about 8.8 hPa and 5.8 hPa respectively. A more comprehensive view of the present circulation patterns and their future changes is presented in Figure 3. At the NH, a poleward shift of the zonal wind at 250 hPa is found during DJF over the Atlantic and the eastern Asia, and an equatorward shift over the NH Central and Eastern Pacific, while at the SH a poleward shift is seen over the Indian Ocean. During JJA, an equatorward shift of the NH subtropical jet stream is depicted over central and eastern Asia, while at the SH a poleward shift is seen over Australia.

The impacts of RCP6.0 emissions scenario on tropopause folds frequency are hereafter investigated, considering as folds all folds with $\Delta p \geq 50$ hPa (shallow, medium and deep). Figure 4 presents the projected fold frequency changes between the FUT and REF periods along with the climatology of fold frequencies during the REF period for every season. The spatial distribution of fold frequencies during the REF period (green contours in Fig. 4), indicates that in principal folds occur in the regions with high zonal wind speed (colour shadings in Fig. 3). Noteworthy are the hotspots over Asia and Middle East during DJF and JJA, and over the southern Indian Ocean during JJA, whereas during the transition seasons the maxima are located over Asia in MAM, and over Asia and southern Indian Ocean in SON, being consistent with the ERA-Interim derived tropopause fold climatology of Škerlak et al. (2015). The projected changes in fold occurrence for the FUT period with respect to the REF period during DJF reveal a a distinct pattern of decrease/increase of folds frequency over south Asia/NH Pacific Ocean, associated with the adjacent decrease/increase of zonal wind in the upper troposphere depicted from Figure 3a. During JJA, the equatorward shift of the subtropical jet stream over central Asia implies in an dipole pattern of decrease/increase in fold frequencies, while in the SH a decrease/increase in fold occurrence is found over Southern Africa/Indian Ocean as a response to the projected changes in the upper tropospheric zonal winds. During MAM a distinct increase in folds frequency prevails in a zone extending across the NH Pacific Ocean, and a decrease at the north of India, while during SON more frequent folding events are projected over the NH Western Pacific Ocean and the Indian Ocean.

https://doi.org/10.5194/acp-2019-508
Preprint. Discussion started: 14 June 2019

Atmospheric Chemistry and Physics Discussions

3.2 Tropospheric ozone

Here we explore the future changes in tropospheric ozone under the RCP6.0 GHGs scenario. Figure 5 presents the projected changes of zonal-mean ozone along with its climatological values during the REF period in a seasonal basis. The highest concentrations of zonal-mean ozone in the troposphere during the REF period are found at the NH mid-latitudes during MAM and JJA and at the SH mid-latitudes during SON. With respect to the REF period, a decrease of zonal-mean ozone in the lower troposphere up to 3 $\mathrm{nmol/mol}$ is projected for the FUT period during MAM and JJA in the NH, and similarly during DJF (austral summer) at the SH, resulting from the RCP6.0 future ozone precursor emissions reduction, which as expected dominates during the seasons with more intense photochemistry. Additionally, even if we have no change in precursor emissions, as has been also outlined in the 5^{th} IPCC Assessment Report (Kirtman et al., 2013), there is high confidence that in unpolluted regions, higher water vapour abundances and temperatures in a warmer climate enhance ozone destruction, leading to lower baseline ozone levels, while there is medium confidence that in polluted regions it is expected to increase surface ozone. Clearly, temperature and humidity under a warmer climate play an important role for lower ozone in the tropical Pacific, due to the increased rate of the ozone destruction reactions (Revell et al., 2015). Contrary, in the extratropical lower stratosphere and the upper and middle troposphere ozone is projected to increase during all seasons. The largest increases in the upper and middle troposphere, of up to 12 $\mathrm{nmol/mol}$, are seen in the subtropics and in the vicinity of the jet streams where tropopause folds formation and the induced STT are favoured. The more pronounced increases of ozone are found in the NH/SH during MAM/SON throughout the entire free troposphere. As regards the lower stratosphere, an increase of ozone is projected outside the tropics reflecting the recovery of stratospheric ozone. In the tropical lower stratosphere, the projected decrease of ozone is presumably related to the BDC strengthening and the induced increased upwelling of tropospheric ozone-poor air into the lower stratosphere. These patterns of tropospheric ozone increase are probably resulting from a global STE increase, linked to stratospheric ozone recovery and a strengthening of BDC, as suggested by previous studies based on simulations with CCMs (Banerjee et al., 2016; Morgenstern et al., 2018). In the free troposphere, it seems that the beneficial reduction of ozone precursor emissions is canceled out by the projected increase of stratospheric ozone influx.

3.3 Stratospheric ozone tracer (O3s)

To estimate the impact of STE on tropospheric ozone, the projected changes of O3s are examined here. Same as in Figure 5, Figure 6 depicts the differences of zonal-mean O3s concentrations between the FUT and REF periods. An increase of O3s occurs almost throughout the troposphere during all seasons. In the NH, the peak of O3s enhancement is found in the subtropics and in the vicinity of the NH jet stream during DJF and MAM (Fig. 6a and c), while in the SH the respective positive maxima are seen during JJA and SON (Fig. 6b and d), similarily near the position of the SH jet stream. These increases of O3s in the NH/SH subtropical upper and middle troposphere, reveal an increase of isentropic cross-tropopause ozone transport, through tropopause folds that in principal occur near the NH/SH subtropical jet streams. In general, the positive O3s patterns resemble that of tropospheric ozone (Fig. 5), indicating that the projected increase of tropospheric ozone is mainly driven by the increase in STT and the induced vertical transport of stratospheric ozone in the underlying troposphere, as it is was also reported from

https://doi.org/10.5194/acp-2019-508
Preprint. Discussion started: 14 June 2019


Atmospheric Chemistry and Physics Discussions

previous modeling studies employing a tracer for stratospheric ozone in future projected sensitivity simulations (Banerjee et al., 2016; Meul et al., 2018). Meul et al. (2018) in their future projected simulations under the RCP8.5 GHGs scenario with the EMAC model noted a similar increase in STE of ozone, which was attributed to the rising GHGs concentrations. A small decrease of O3s occurring mainly in the SH/NH lower troposphere during DJF/JJA, is associated with an increased chemical O3s loss due to a slight increase in OH and HO_2 and their reaction rate with ozone (due to increased temperature).

The spatial distribution of O3s projected changes at 400 hPa is presented in Figure 7, to identify the global hot spots of climate change impact on ozone STT. Overall, an increase of ozone with stratospheric origin is projected in the middle troposphere (400 hPa) during all seasons, reflecting the recovery of stratospheric ozone and the associated increase of ozone STE. Notably, the maxima of O3s increase coincides mainly with the respective maxima of tropopause folds frequency increase (see Fig. 4). In more detail, during DJF the peaks of future O3s increases (up to 12 $\mathrm{nmol/mol}$) are found over the NH Pacific Ocean (Fig. 7a), while during JJA the respective peaks (exceeding 12 $\mathrm{nmol/mol}$) are mainly occured over the central Asia and the Indian Ocean (Fig. 7c). All in all, the emerging increase in ozone STE under the RCP6.0 GHGs scenario is mainly driven by the recovery of stratospheric ozone, still for regions where tropopause folds are projected to occur more often, the downward transport of ozone from the stratosphere seems to be more pronounced.

4 Hot spots of ozone STT

STT is of great importance for ozone levels and variability in the upper/middle troposphere over regions where the meteorological conditions favor the formation of tropopause folds and the downward transport (Roelofs and Lelieveld, 1997; Sprenger and Wernli, 2003), such as the eastern Mediterranean and the Middle East (EMME) (Li et al., 2001; Zanis et al., 2014; Akritidis et al., 2016), and the broader Afghanistan area (AFG) (Tyrlis et al., 2014; Ojha et al., 2017) during summer, and especially the July-August period. To explore the links of the tropopause folds frequency and stratospheric ozone, with the interannual variability of middle tropospheric ozone with stratospheric origin over the EM (20-45°E,30-40°N) and AFG (60-80°E, 30-40°N) regions, the mean July-August timeseries of tropopause folds frequency, ozone at 150 hPa, and O3s at 400 and 500 hPa for the period 1960-2099 were constructed. Figure 8a presents the mean July-August fields of tropopause folds frequency during the REF period revealing a pronounced fold activity over the depicted EM and AFG regions. For the EM region (Fig. 8b), the interannual variability of mean July-August O3s at 400 hPa (500 hPa) is found to be positevely correlated at the 99% significance level with the mean July-August tropopause folds frequency and ozone at 150 hPa, with values of r=0.53 (r=0.43) and r=0.56 (r=0.49), respectively. Employing a multiple linear regression analysis, folds frequency and ozone at 150 hPa are found to explain the 58% (42%) of the variance of O3s at 400 hPa (500 hPa). As regards the AFG region, the variance of the projected mean July-August O3s concentrations at 400 hPa (500 hPa) explained by folds frequency and ozone at 150 hPa is 73% (68%). The year-to-year variability of July-August O3s at 400 hPa (500 hPa) is found positevely correlated at the 99% significance level with both fold frequency r=0.64 (r=0.58) and ozone at 150 hPa r=0.64 (r=0.64).

https://doi.org/10.5194/acp-2019-508
Preprint. Discussion started: 14 June 2019

Atmospheric Chemistry and Physics Discussions

5 Conclusions

This study investigates the future projected changes in tropopause folds, ozone STT and tropospheric ozone under the RCP6.0 emissions scenario, using a transient simulation with EMAC CCM from 1960 to 2100 and a tropopause fold identification algorithm. In particular, we examined the long-term change in tropopause folds frequency and the potential links with atmospheric circulation changes. Moreover, the long-term changes in tropospheric ozone and ozone STT were also explored and associated with the respective variations in fold activity. The most noteworthy findings of the present study can be summarized as follows:

- Robust changes in atmospheric circulation are identified under the RCP6.0 GHGs emissions scenario. A poleward and upward shift of the NH subtropical jet is projected for DJF and SON, while a strengthening of zonal-mean wind in the upper troposphere is seen equatorward for JJA. The responses are more pronounced at the SH showing a distinct poleward shift for DJF and MAM, with a strengthening of zonal-mean wind poleward during JJA and SON.

- The spatial patterns of the projected changes in NH and SH subtropical jets seem to drive the respective patterns of tropopause folds frequency future changes, with a negative/positive dipole structure found over south Asia/NH Pacific Ocean during DJF and MAM. The most prominent features during JJA are a distinct increase of fold activity over the Indian Ocean exceeding 3%, and a negative/positive dipole structure centered over the greater Afghanistan region.

- The regions exhibiting the highest increases in tropopause folds occurrence in future are those with the more pronounced projected increases of O3s in the middle troposphere (400 hPa). The projected changes of zonal-mean O3s concentrations reveal a strengthening of ozone STT at the middle latitudes of both hemispheres during all seasons, which is more distinct at the NH during DJF and MAM (up to 6 $\mathrm{nmol/mol}$ down to 500 hPa), and at the SH during JJA and SON (up to 8 nmol/mol down to 500 hPa). Although the future increase in ozone STT on a global scale seems to be forced from stratospheric ozone recovery and strengthening of BDC (Banerjee et al., 2016; Meul et al., 2018), regionally, the degree of increase in the downward transport of stratospheric ozone is partially driven from the long-term changes of fold activity.

- For specific regions considered as global STT hotspots, namely the summertime EMME and AFG, the projected year-to-year variability of middle tropospheric ozone with stratospheric origin seems to be largely governed from both the variabilities of ozone at 150 hPa and folds frequency, as they explain 60% and 68% of the variance of mean July-August O3s concentrations at 400 hPa for EMME and AFG respectively, over the period 1960-2100.

- Ozone in the lower troposphere and near the surface decreases under the projected decline in ozone precursors emissions during MAM and JJA at the NH, and during DJF at the SH, as photochemical ozone production is more dominant during these seasons. In the middle and upper troposphere the projected strengthening of ozone STT results in a distinct increase of ozone globally, that seems to cancel out the aforementioned ozone decrease due to emissions reduction.

https://doi.org/10.5194/acp-2019-508
Preprint. Discussion started: 14 June 2019

Atmospheric Chemistry and Physics Discussions

In summary, the findings of this study are in the same direction with other studies based in different CCMs (Zeng et al., 2010; Banerjee et al., 2016; Meul et al., 2018), increasing confidence in the direction of an increased ozone STT and induced increases in middle/upper tropospheric ozone in the future under the RCP6.0 emissions scenario. The role of tropopause folds activity in a changing climate seems to be a considerable factor for both the levels and variability of ozone STT.

Author contributions. DA performed the analysis and wrote the paper with contributions from PZ and AP. AP provided the EMAC model data. PZ and AP contributed to the interpretation of the results.

Competing interests. The authors declare that they have no conflict of interest.

Acknowledgement. The EMAC model simulations were performed at the German Climate Computing Center (DKRZ) with support from the Bundesministerium für Bildung und Forschung (BMBF). The authors gratefully acknowledge DKRZ and its scientific steering committee for providing the HPC and data archiving resources for the consortial project ESCiMo (Earth System Chemistry integrated Modelling). The authors are furthermore grateful to Patrick Jöckel for his contribution to the ESCiMo simulations and the EMAC model development. The authors also acknowledge Michael Sprenger (ETH Zurich) for the development of the 3-D labeling algorithm, which is used in the present study for the detection of tropopause folds in EMAC simulation. Dimitris Akritidis aknowledges the Research Committee of the Aristotle University of Thessaloniki (https://www.rc.auth.gr) for the 2015 Postdoctoral Excellence Fellowship.

https://doi.org/10.5194/acp-2019-508
Preprint. Discussion started: 14 June 2019

Atmospheric Chemistry and Physics Discussions

References

Akritidis, D., Zanis, P., Pytharoulis, I., Mavrakis, A., and Karacostas, T.: A deep stratospheric intrusion event down to the earth's surface of the megacity of Athens, Meteorology and atmospheric physics, 109, 9–18, 2010.

Akritidis, D., Pozzer, A., Zanis, P., Tyrlis, E., Škerlak, B., Sprenger, M., and Lelieveld, J.: On the role of tropopause folds in summertime tropospheric ozone over the eastern Mediterranean and the Middle East, Atmos. Chem. Phys, 16, 14 025–14 039, 2016.

Astitha, M., Lelieveld, J., Abdel Kader, M., Pozzer, A., and Meij, A. d.: Parameterization of dust emissions in the global atmospheric chemistry-climate model EMAC: impact of nudging and soil properties, Atmospheric Chemistry and Physics, 12, 11 057–11 083, 2012.

Banerjee, A., Maycock, A. C., Archibald, A. T., Abraham, N. L., Telford, P., Braesicke, P., and Pyle, J. A.: Drivers of changes in stratospheric and tropospheric ozone between year 2000 and 2100, Atmospheric Chemistry and Physics, 16, 2727–2746, https://doi.org/10.5194/acp-16-2727-2016, 2016.

Butler, A. H., Thompson, D. W. J., and Heikes, R.: The Steady-State Atmospheric Circulation Response to Climate Change–like Thermal Forcings in a Simple General Circulation Model, Journal of Climate, 23, 3474–3496, https://doi.org/10.1175/2010JCLI3228.1, 2010.

Carpenter, L., Reimann, S., Burkholder, J., Clerbaux, C., Hall, B., Hossaini, R., Laube, J., and Yvon-Lewis, S.: Scientific Assessment of Ozone Depletion: 2014, 2014.

Collins, W., Bellouin, N., Doutriaux-Boucher, M., Gedney, N., Halloran, P., Hinton, T., Hughes, J., Jones, C., Joshi, M., Liddicoat, S., et al.: Development and evaluation of an Earth-System model–HadGEM2, Geoscientific Model Development, 4, 1051–1075, 2011.

Cristofanelli, P., Bonasoni, P., Tositti, L., Bonafe, U., Calzolari, F., Evangelisti, F., Sandrini, S., and Stohl, A.: A 6-year analysis of stratospheric intrusions and their influence on ozone at Mt. Cimone (2165 m above sea level), Journal of Geophysical Research: Atmospheres, 111, 2006.

Dee, D., Uppala, S., Simmons, A., Berrisford, P., Poli, P., Kobayashi, S., Andrae, U., Balmaseda, M., Balsamo, G., Bauer, P., et al.: The ERA-Interim reanalysis: Configuration and performance of the data assimilation system, Quarterly Journal of the Royal Meteorological Society, 137, 553–597, 2011.

Delcambre, S. C., Lorenz, D. J., Vimont, D. J., and Martin, J. E.: Diagnosing Northern Hemisphere Jet Portrayal in 17 CMIP3 Global Climate Models: Twenty-First-Century Projections, Journal of Climate, 26, 4930–4946, https://doi.org/10.1175/JCLI-D-12-00359.1, 2013.

Doherty, R. M., Orbe, C., Zeng, G., Plummer, D. A., Prather, M. J., Wild, O., Lin, M., Shindell, D. T., and Mackenzie, I. A.: Multi-model impacts of climate change on pollution transport from global emission source regions, Atmospheric Chemistry and Physics, 17, 14 219–14 237, https://doi.org/10.5194/acp-17-14219-2017, https://www.atmos-chem-phys.net/17/14219/2017/, 2017.

Eyring, V., Lamarque, J.-F., Hess, P., Arfeuille, F., Bowman, K., Chipperfiel, M. P., Duncan, B., Fiore, A., Gettelman, A., Giorgetta, M. A., et al.: Overview of IGAC/SPARC Chemistry-Climate Model Initiative (CCMI) community simulations in support of upcoming ozone and climate assessments, Sparc Newsletter, 40, 48–66, 2013.

Fiore, A. M., Naik, V., and Leibensperger, E. M.: Air Quality and Climate Connections, Journal of the Air & Waste Management Association, 65, 645–685, https://doi.org/10.1080/10962247.2015.1040526, 2015.

Fujino, J., Nair, R., Kainuma, M., Masui, T., and Matsuoka, Y.: Multi-gas mitigation analysis on stabilization scenarios using AIM global model, The Energy Journal, pp. 343–353, 2006.

Hardiman, S. C., Butchart, N., and Calvo, N.: The morphology of the Brewer-Dobson circulation and its response to climate change in CMIP5 simulations, Quarterly Journal of the Royal Meteorological Society, 140, 2014.

https://doi.org/10.5194/acp-2019-508
Preprint. Discussion started: 14 June 2019

Hess, P., Kinnison, D., and Tang, Q.: Ensemble simulations of the role of the stratosphere in the attribution of northern extratropical tropospheric ozone variability, Atmospheric Chemistry and Physics, 15, 2341–2365, https://doi.org/10.5194/acp-15-2341-2015, 2015.

Holton, J. R., Haynes, P. H., McIntyre, M. E., Douglass, A. R., Rood, R. B., and Pfister, L.: Stratosphere-troposphere exchange, Reviews of Geophysics, 33, 403–439, 1995.

Hoskins, B. J., McIntyre, M., and Robertson, A. W.: On the use and significance of isentropic potential vorticity maps, Quarterly Journal of the Royal Meteorological Society, 111, 877–946, 1985.

Jöckel, P., Kerkweg, A., Pozzer, A., Sander, R., Tost, H., Riede, H., Baumgaertner, A., Gromov, S., and Kern, B.: Development cycle 2 of the Modular Earth Submodel System (MESSy2), Geoscientific Model Development, 3, 717–752, https://doi.org/10.5194/gmd-3-717-2010, 2010.

Jöckel, P., Tost, H., Pozzer, A., Kunze, M., Kirner, O., Brenninkmeijer, C. A., Brinkop, S., Cai, D. S., Dyroff, C., Eckstein, J., et al.: Earth System Chemistry integrated Modelling (ESCiMo) with the Modular Earth Submodel System (MESSy) version 2.51., Geoscientific Model Development, 9, 2016.

Kirtman, B., Power, S., Adedoyin, A., Boer, G., Bojariu, R., Camilloni, I., Doblas-Reyes, F., Fiore, A., Kimoto, M., Meehl, G., et al.: Near-term climate change: projections and predictability, 2013.

Knowland, K., Ott, L., Duncan, B., and Wargan, K.: Stratospheric Intrusion-Influenced Ozone Air Quality Exceedances Investigated in the NASA MERRA-2 Reanalysis, Geophysical Research Letters, 44, 2017.

Lamarque, J.-F., Bond, T. C., Eyring, V., Granier, C., Heil, A., Klimont, Z., Lee, D., Liousse, C., Mieville, A., Owen, B., et al.: Historical (1850–2000) gridded anthropogenic and biomass burning emissions of reactive gases and aerosols: methodology and application, Atmospheric Chemistry and Physics, 10, 7017–7039, 2010.

Lefohn, A. S., Emery, C., Shadwick, D., Wernli, H., Jung, J., and Oltmans, S. J.: Estimates of background surface ozone concentrations in the United States based on model-derived source apportionment, Atmospheric environment, 84, 275–288, 2014.

Lelieveld, J., Gromov, S., Pozzer, A., and Taraborrelli, D.: Global tropospheric hydroxyl distribution, budget and reactivity, Atmospheric Chemistry and Physics, 16, 12 477–12 493, https://doi.org/10.5194/acp-16-12477-2016, https://www.atmos-chem-phys.net/16/12477/2016/, 2016.

Li, Q., Jacob, D. J., Logan, J. A., Bey, I., Yantosca, R. M., Liu, H., Martin, R. V., Fiore, A. M., Field, B. D., Duncan, B. N., and Thouret, V.: A tropospheric ozone maximum over the Middle East, Geophysical Research Letters, 28, 3235–3238, https://doi.org/10.1029/2001GL013134, 2001.

Lin, M., Fiore, A. M., Cooper, O. R., Horowitz, L. W., Langford, A. O., Levy, H., Johnson, B. J., Naik, V., Oltmans, S. J., and Senff, C. J.: Springtime high surface ozone events over the western United States: Quantifying the role of stratospheric intrusions, Journal of Geophysical Research: Atmospheres, 117, 2012.

Lin, M., Fiore, A. M., Horowitz, L. W., Langford, A. O., Oltmans, S. J., Tarasick, D., and Rieder, H. E.: Climate variability modulates western US ozone air quality in spring via deep stratospheric intrusions, Nature communications, 6, 2015.

Lorenz, D. J. and DeWeaver, E. T.: Tropopause height and zonal wind response to global warming in the IPCC scenario integrations, Journal of Geophysical Research: Atmospheres, 112, https://doi.org/10.1029/2006JD008087, 2007.

Martin, T. H. D. T. G. M., Bellouin, N., Collins, W. J., Culverwell, I. D., Halloran, P. R., Hardiman, S. C., Hinton, T. J., Jones, C. D., McDonald, R. E., McLaren, A. J., O'Connor, F. M., Roberts, M. J., Rodriguez, J. M., Woodward, S., Best, M. J., Brooks, M. E., Brown, A. R., Butchart, N., Dearden, C., Derbyshire, S. H., Dharssi, I., Doutriaux-Boucher, M., Edwards, J. M., Falloon, P. D., Gedney, N., Gray, L. J., Hewitt, H. T., Hobson, M., Huddleston, M. R., Hughes, J., Ineson, S., Ingram, W. J., James, P. M., Johns, T. C., Johnson, C. E.,

https://doi.org/10.5194/acp-2019-508
Preprint. Discussion started: 14 June 2019

Jones, A., Jones, C. P., Joshi, M. M., Keen, A. B., Liddicoat, S., Lock, A. P., Maidens, A. V., Manners, J. C., Milton, S. F., Rae, J. G. L., Ridley, J. K., Sellar, A., Senior, C. A., Totterdell, I. J., Verhoef, A., Vidale, P. L., and Wiltshire, A.: The HadGEM2 family of Met Office Unified Model climate configurations, Geoscientific Model Development, 4, 723–757, https://doi.org/10.5194/gmd-4-723-2011, 2011.

Meul, S., Langematz, U., Kröger, P., Oberländer-Hayn, S., and Jöckel, P.: Future changes in the stratosphere-to-troposphere ozone mass flux and the contribution from climate change and ozone recovery, Atmospheric Chemistry and Physics, 18, 7721–7738, https://doi.org/10.5194/acp-18-7721-2018, 2018.

Monks, P. S., Archibald, A. T., Colette, A., Cooper, O., Coyle, M., Derwent, R., Fowler, D., Granier, C., Law, K. S., Mills, G. E., Stevenson, D. S., Tarasova, O., Thouret, V., von Schneidemesser, E., Sommariva, R., Wild, O., and Williams, M. L.: Tropospheric ozone and its precursors from the urban to the global scale from air quality to short-lived climate forcer, Atmospheric Chemistry and Physics, 15, 8889–8973, https://doi.org/10.5194/acp-15-8889-2015, https://www.atmos-chem-phys.net/15/8889/2015/, 2015.

Morgenstern, O., Stone, K. A., Schofield, R., Akiyoshi, H., Yamashita, Y., Kinnison, D. E., Garcia, R. R., Sudo, K., Plummer, D. A., Scinocca, J., Oman, L. D., Manyin, M. E., Zeng, G., Rozanov, E., Stenke, A., Revell, L. E., Pitari, G., Mancini, E., Di Genova, G., Visioni, D., Dhomse, S. S., and Chipperfield, M. P.: Ozone sensitivity to varying greenhouse gases and ozone-depleting substances in CCMI-1 simulations, Atmospheric Chemistry and Physics, 18, 1091–1114, https://doi.org/10.5194/acp-18-1091-2018, 2018.

Naik, V., Voulgarakis, A., Fiore, A. M., Horowitz, L. W., Lamarque, J.-F., Lin, M., Prather, M. J., Young, P. J., Bergmann, D., Cameron-Smith, P. J., Cionni, I., Collins, W. J., Dalsøren, S. B., Doherty, R., Eyring, V., Faluvegi, G., Folberth, G. A., Josse, B., Lee, Y. H., MacKenzie, I. A., Nagashima, T., van Noije, T. P. C., Plummer, D. A., Righi, M., Rumbold, S. T., Skeie, R., Shindell, D. T., Stevenson, D. S., Strode, S., Sudo, K., Szopa, S., and Zeng, G.: Preindustrial to present day changes in tropospheric hydroxyl radical and methane lifetime from the Atmospheric Chemistry and Climate Model Intercomparison Project (ACCMIP), Atmos. Chem. Phys., 13, 5277–5298, https://doi.org/10.5194/acp-13-5277-2013, 2013.

Neu, J. L., Flury, T., Manney, G. L., Santee, M. L., Livesey, N. J., and Worden, J.: Tropospheric ozone variations governed by changes in stratospheric circulation, Nature Geoscience, 7, 340, https://doi.org/10.1038/ngeo2138, 2014.

Oberländer-Hayn, S., Gerber, E. P., Abalichin, J., Akiyoshi, H., Kerschbaumer, A., Kubin, A., Kunze, M., Langematz, U., Meul, S., Michou, M., Morgenstern, O., and Oman, L. D.: Is the Brewer-Dobson circulation increasing or moving upward?, Geophysical Research Letters, 43, 1772–1779, https://doi.org/10.1002/2015GL067545, https://agupubs.onlinelibrary.wiley.com/doi/abs/10.1002/2015GL067545, 2016.

Ojha, N., Pozzer, A., Akritidis, D., and Lelieveld, J.: Secondary ozone peaks in the troposphere over the Himalayas, Atmospheric Chemistry and Physics, 17, 6743–6757, https://doi.org/10.5194/acp-17-6743-2017, https://www.atmos-chem-phys.net/17/6743/2017/, 2017.

Orbe, C., Newman, P. A., Waugh, D. W., Holzer, M., Oman, L. D., Li, F., and Polvani, L. M.: Air-mass origin in the Arctic. Part II: Response to increases in greenhouse gases, Journal of Climate, 28, 9105–9120, 2015.

Palmeiro, F. M., Calvo, N., and Garcia, R. R.: Future Changes in the Brewer–Dobson Circulation under Different Greenhouse Gas Concentrations in WACCM4, Journal of the Atmospheric Sciences, 71, 2962–2975, https://doi.org/10.1175/JAS-D-13-0289.1, 2014.

Pozzer, A., Jöckel, P., Tost, H., Sander, R., Ganzeveld, L., Kerkweg, A., and Lelieveld, J.: Simulating organic species with the global atmospheric chemistry general circulation model ECHAM5/MESSy1: a comparison of model results with observations, Atmospheric Chemistry and Physics, 7, 2527–2550, 2007.

Pozzer, A., Meij, A. d., Pringle, K., Tost, H., Doering, U., Aardenne, J. v., and Lelieveld, J.: Distributions and regional budgets of aerosols and their precursors simulated with the EMAC chemistry-climate model, Atmospheric Chemistry and Physics, 12, 961–987, 2012.

Pringle, K., Tost, H., Metzger, S., Steil, B., Giannadaki, D., Nenes, A., Fountoukis, C., Stier, P., Vignati, E., and Lelieveld, J.: Description and evaluation of GMXe: a new aerosol submodel for global simulations (v1), Geosci. Model Dev., 3, 391–412, 2010.

https://doi.org/10.5194/acp-2019-508
Preprint. Discussion started: 14 June 2019

Revell, L. E., Tummon, F., Salawitch, R. J., Stenke, A., and Peter, T.: The changing ozone depletion potential of N2O in a future climate, Geophysical Research Letters, 42, 10,047–10,055, https://doi.org/10.1002/2015GL065702, 2015.

Roeckner, E., Brokopf, R., Esch, M., Giorgetta, M., Hagemann, S., Kornblueh, L., Manzini, E., Schlese, U., and Schulzweida, U.: Sensitivity of simulated climate to horizontal and vertical resolution in the ECHAM5 atmosphere model, Journal of Climate, 19, 3771–3791, 2006.

Roelofs, G.-J. and Lelieveld, J.: Model study of the influence of cross-tropopause O3 transports on tropospheric O3 levels, Tellus B, 49, 38–55, 1997.

Sekiya, T. and Sudo, K.: Roles of transport and chemistry processes in global ozone change on interannual and multidecadal time scales, 2014.

Škerlak, B., Sprenger, M., Pfahl, S., Tyrlis, E., and Wernli, H.: Tropopause Folds in ERA-Interim: Global Climatology and Relation to Extreme Weather Events, Journal of Geophysical Research: Atmospheres, 2015.

Sprenger, M. and Wernli, H.: A Northern Hemispheric climatology of cross-tropopause exchange for the ERA15 time period (1979–1993), Journal of Geophysical Research: Atmospheres (1984–2012), 108, 2003.

Sprenger, M., Croci Maspoli, M., and Wernli, H.: Tropopause folds and cross-tropopause exchange: A global investigation based upon ECMWF analyses for the time period March 2000 to February 2001, Journal of Geophysical Research: Atmospheres (1984–2012), 108, 2003.

Stevenson, D. S., Dentener, F. J., Schultz, M. G., Ellingsen, K., van Noije, T. P. C., Wild, O., Zeng, G., Amann, M., Atherton, C. S., Bell, N., Bergmann, D. J., Bey, I., Butler, T., Cofala, J., Collins, W. J., Derwent, R. G., Doherty, R. M., Drevet, J., Eskes, H. J., Fiore, A. M., Gauss, M., Hauglustaine, D. A., Horowitz, L. W., Isaksen, I. S. A., Krol, M. C., Lamarque, J.-F., Lawrence, M. G., Montanaro, V., Müller, J.-F., Pitari, G., Prather, M. J., Pyle, J. A., Rast, S., Rodriguez, J. M., Sanderson, M. G., Savage, N. H., Shindell, D. T., Strahan, S. E., Sudo, K., and Szopa, S.: Multimodel ensemble simulations of present-day and near-future tropospheric ozone, J. Geophys. Res., 111, D08 301, https://doi.org/10.1029/2005JD006338, 2006.

Stohl, A., Bonasoni, P., Cristofanelli, P., Collins, W., Feichter, J., Frank, A., Forster, C., Gerasopoulos, E., Gaggeler, H., James, P., Kentarchos, T., Kromp-Kolb, H., KrÃ¼ger, B., Land, C., Meloen, J., Papayannis, A., Priller, A., Seibert, P., Sprenger, M., Roelofs, G. J., Scheel, H. E., Schnabel, C., Siegmund, P., Tobler, L., Trickl, T., Wernli, H., Wirth, V., Zanis, P., and Zerefos, C.: Stratosphere-troposphere exchange: A review, and what we have learned from STACCATO, Journal of Geophysical Research: Atmospheres, 108, https://doi.org/10.1029/2002JD002490, 2003.

Swart, N. C. and Fyfe, J. C.: Observed and simulated changes in the Southern Hemisphere surface westerly wind-stress, Geophysical Research Letters, 39, https://doi.org/10.1029/2012GL052810, 2012.

Tyrlis, E., Škerlak, B., Sprenger, M., Wernli, H., Zittis, G., and Lelieveld, J.: On the linkage between the Asian summer monsoon and tropopause fold activity over the eastern Mediterranean and the Middle East, Journal of Geophysical Research: Atmospheres, 119, 3202–3221, 2014.

Williams, R. S., Hegglin, M. I., Kerridge, B. J., Jöckel, P., Latter, B. G., and Plummer, D. A.: Characterising the seasonal and geographical variability in tropospheric ozone, stratospheric influence and recent changes, Atmospheric Chemistry and Physics, 19, 3589–3620, https://doi.org/10.5194/acp-19-3589-2019, https://www.atmos-chem-phys.net/19/3589/2019/, 2019.

WMO: Guide to climatological practices, World Meteorological Organization, Geneva, 2011.

Yim, B. Y., Min, H. S., and Kug, J.-S.: Inter-model diversity in jet stream changes and its relation to Arctic climate in CMIP5, Climate Dynamics, 47, 235–248, https://doi.org/10.1007/s00382-015-2833-5, 2016.

https://doi.org/10.5194/acp-2019-508
Preprint. Discussion started: 14 June 2019

Atmospheric Chemistry and Physics Discussions

Young, P. J., Archibald, A. T., Bowman, K. W., Lamarque, J.-F., Naik, V., Stevenson, D. S., Tilmes, S., Voulgarakis, A., Wild, O., Bergmann, D., Cameron-Smith, P., Cionni, I., Collins, W. J., Dalsøren, S. B., Doherty, R. M., Eyring, V., Faluvegi, G., Horowitz, L. W., Josse, B., Lee, Y. H., MacKenzie, I. A., Nagashima, T., Plummer, D. A., Righi, M., Rumbold, S. T., Skeie, R. B., Shindell, D. T., Strode, S. A., Sudo, K., Szopa, S., and Zeng, G.: Pre-industrial to end 21st century projections of tropospheric ozone from the Atmospheric Chemistry and Climate Model Intercomparison Project (ACCMIP), Atmospheric Chemistry and Physics, 13, 2063–2090, https://doi.org/10.5194/acp-13-2063-2013, https://www.atmos-chem-phys.net/13/2063/2013/, 2013.

Zanis, P., Hadjinicolaou, P., Pozzer, A., Tyrlis, E., Dafka, S., Mihalopoulos, N., and Lelieveld, J.: Summertime free-tropospheric ozone pool over the eastern Mediterranean/Middle East, Atmospheric Chemistry and Physics, 14, 115–132, 2014.

Zeng, G., Morgenstern, O., Braesicke, P., and Pyle, J. A.: Impact of stratospheric ozone recovery on tropospheric ozone and its budget, Geophysical Research Letters, 37, https://doi.org/10.1029/2010GL042812, https://agupubs.onlinelibrary.wiley.com/doi/abs/10.1029/2010GL042812, 2010.

Zhang, L., Jacob, D. J., Downey, N. V., Wood, D. A., Blewitt, D., Carouge, C. C., van Donkelaar, A., Jones, D. B., Murray, L. T., and Wang, Y.: Improved estimate of the policy-relevant background ozone in the United States using the GEOS-Chem global model with 1/2× 2/3 horizontal resolution over North America, Atmospheric Environment, 45, 6769–6776, 2011.

https://doi.org/10.5194/acp-2019-508
Preprint. Discussion started: 14 June 2019

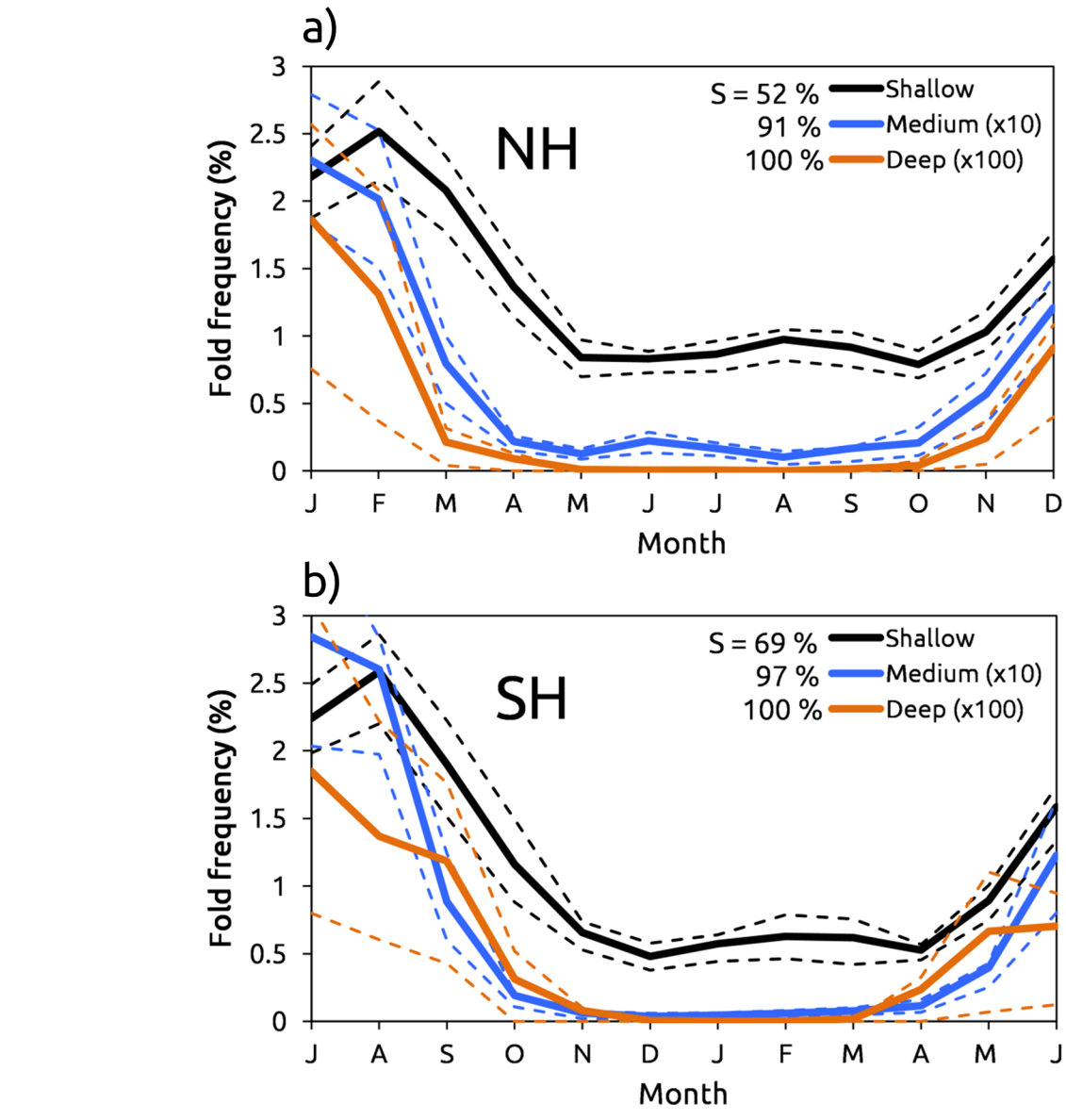

Figure 1. Seasonal cycle of tropopause fold frequencies (%) for (a) the NH (0-65°N) and (b) the SH (0-65°S) over the period 1979-2012 for intercomparison with Figure 7 from Škerlak et al. (2015). The solid lines stand for the mean values, while the dashed coloured lines stand for the 25% and 75% percentiles. The seasonality $S = \frac{max-min}{max+min}$ of each seasonal cycle is also shown.

https://doi.org/10.5194/acp-2019-508
Preprint. Discussion started: 14 June 2019

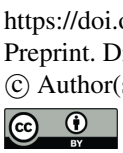

Atmospheric Chemistry and Physics Discussions

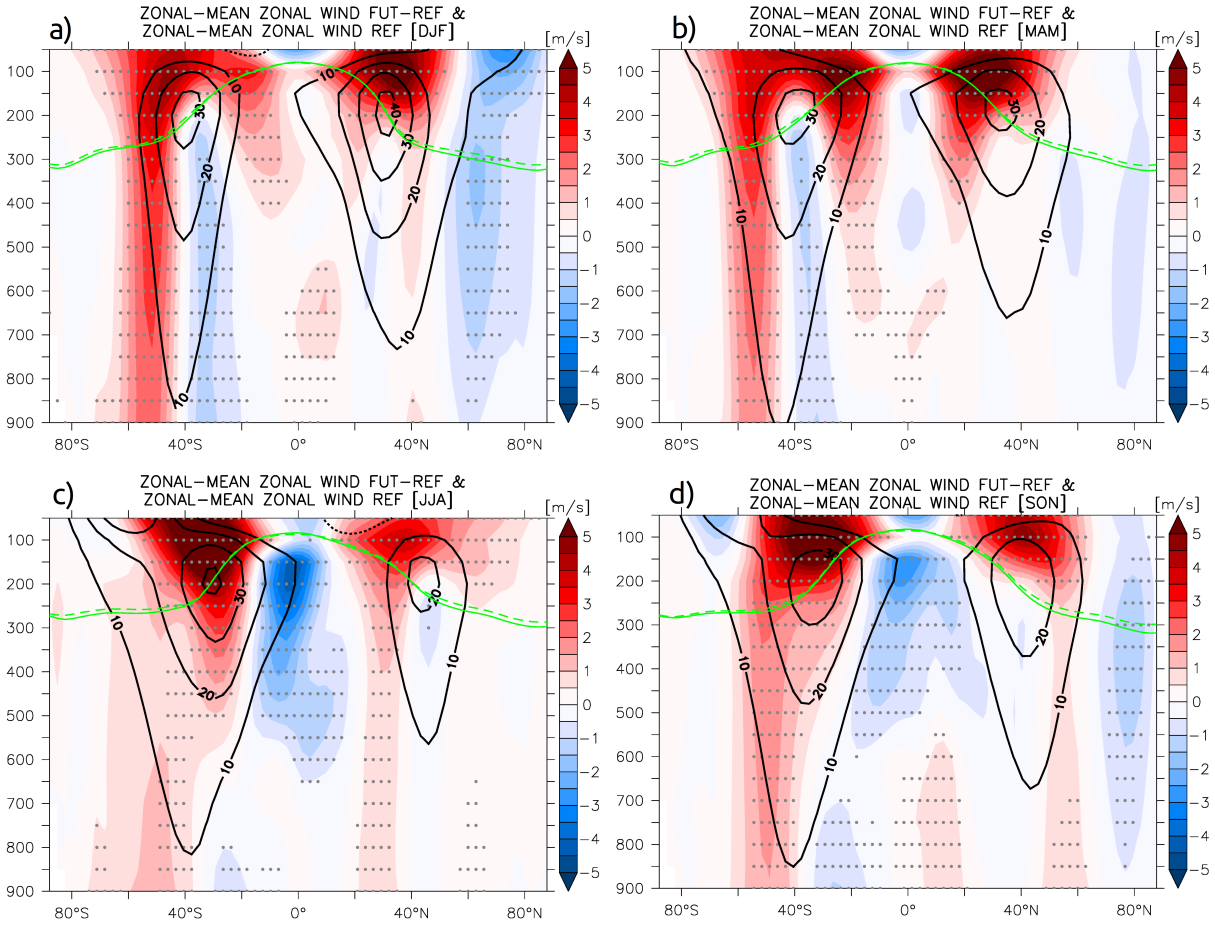

Figure 2. Zonal-mean zonal wind differences between the FUT and REF periods for DJF (a), MAM (b), JJA (c) and SON (d). The black contours indicate the zonal-mean zonal wind climatology for the REF period. The green solid/dashed line denotes the height of the tropopause during the REF/FUT period. Grey dots denote statistically significant changes at the 99% confidence level.

https://doi.org/10.5194/acp-2019-508
Preprint. Discussion started: 14 June 2019

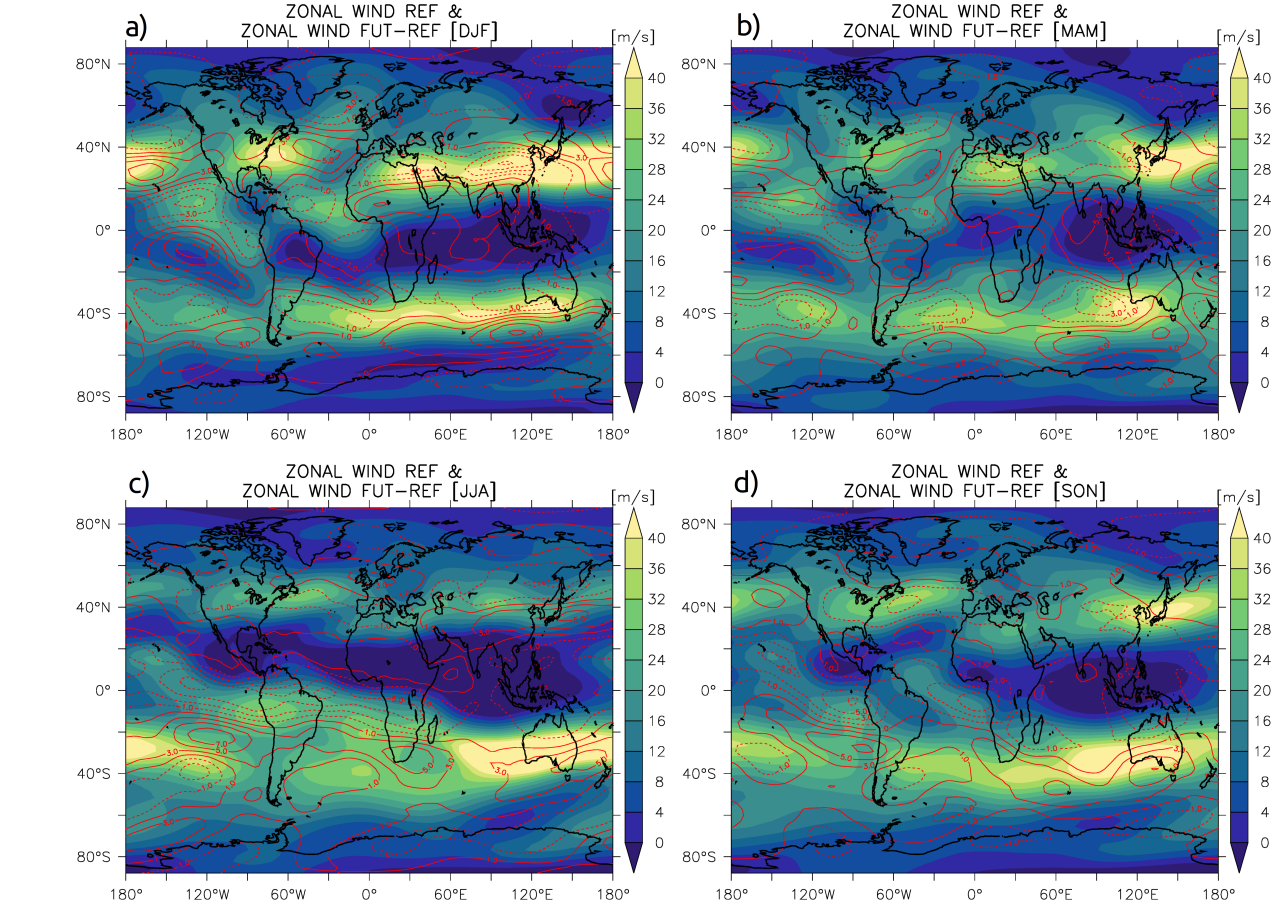

Figure 3. Mean zonal wind at 250 hPa (shaded; m/s) during the REF period for DJF (a), MAM (b), JJA (c) and SON (d). The red contours represent the mean zonal wind differences between the FUT and REF periods.

https://doi.org/10.5194/acp-2019-508
Preprint. Discussion started: 14 June 2019

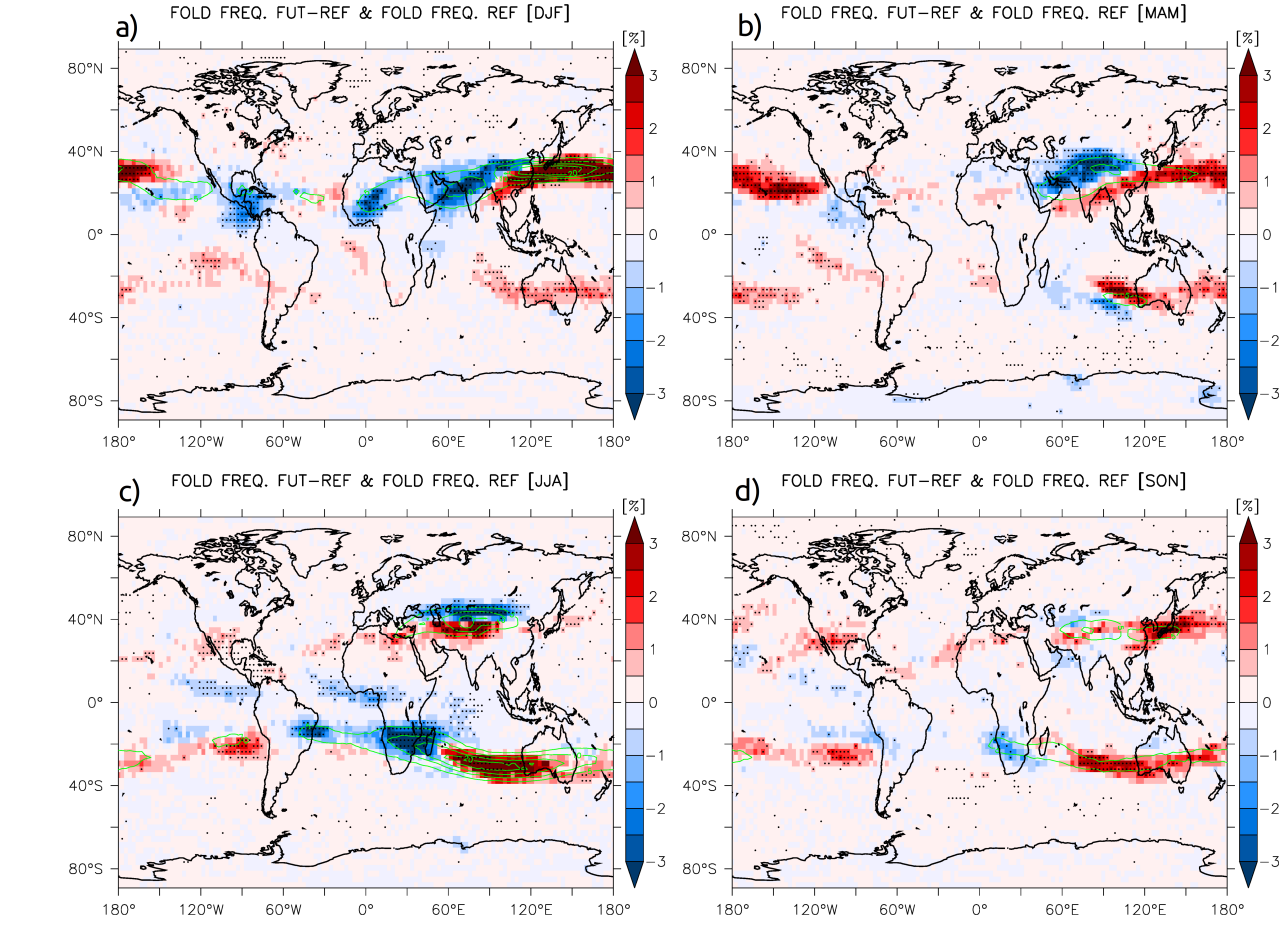

Figure 4. Mean tropopause folds frequency differences (shaded; %) between the FUT and REF period for DJF (a), MAM (b), JJA (c) and SON (d). The black contours denote the tropopause folds frequency during the REF period. The regions where the changes are statistically significant at the 99% confidence level are hatched with black circles.

https://doi.org/10.5194/acp-2019-508
Preprint. Discussion started: 14 June 2019

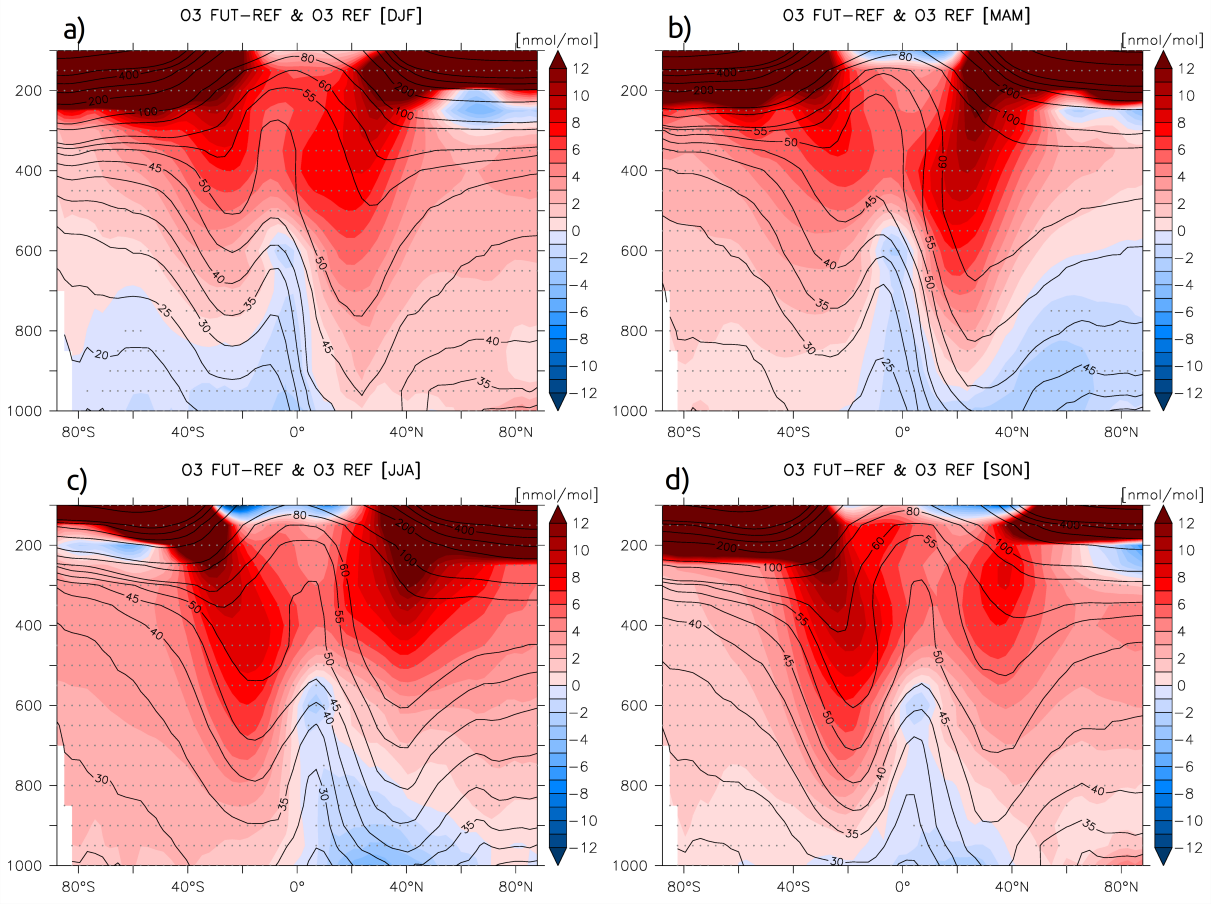

Figure 5. Differences of zonal-mean ozone concentrations between the FUT and REF periods (shaded; nmol/mol) for DJF (a), MAM (b), JJA (c) and SON (d). The black contours denote the zonal-mean ozone concentrations during the REF period. Grey dots denote statistically significant changes at the 99% confidence level.

https://doi.org/10.5194/acp-2019-508
Preprint. Discussion started: 14 June 2019

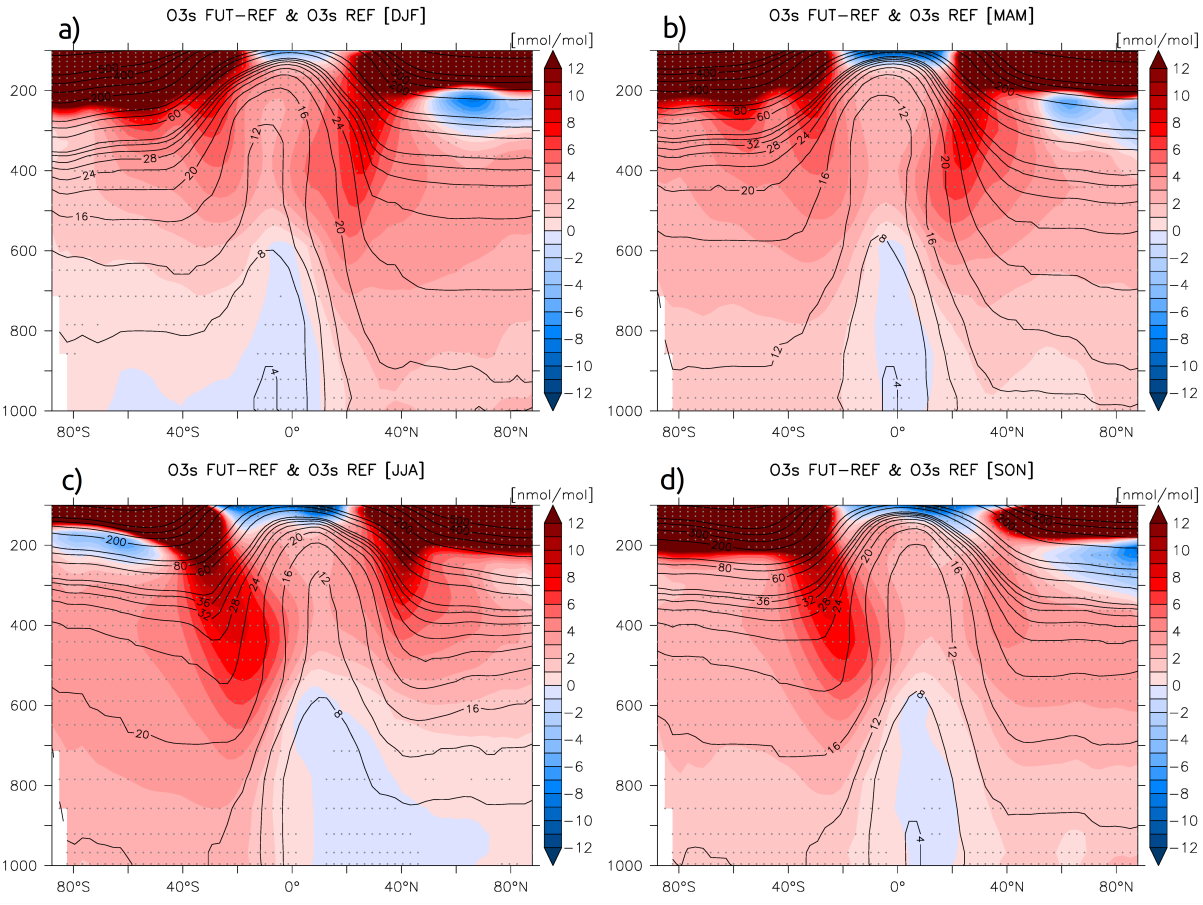

Figure 6. Differences of zonal-mean stratospheric ozone tracer (O3s) concentrations between the FUT and REF periods (shaded; nmol/mol) for DJF (a), MAM (b), JJA (c) and SON (d). The black contours denote the zonal-mean stratospheric ozone tracer concentrations during the REF period. Grey dots denote statistically significant changes at the 99% confidence level.

https://doi.org/10.5194/acp-2019-508
Preprint. Discussion started: 14 June 2019

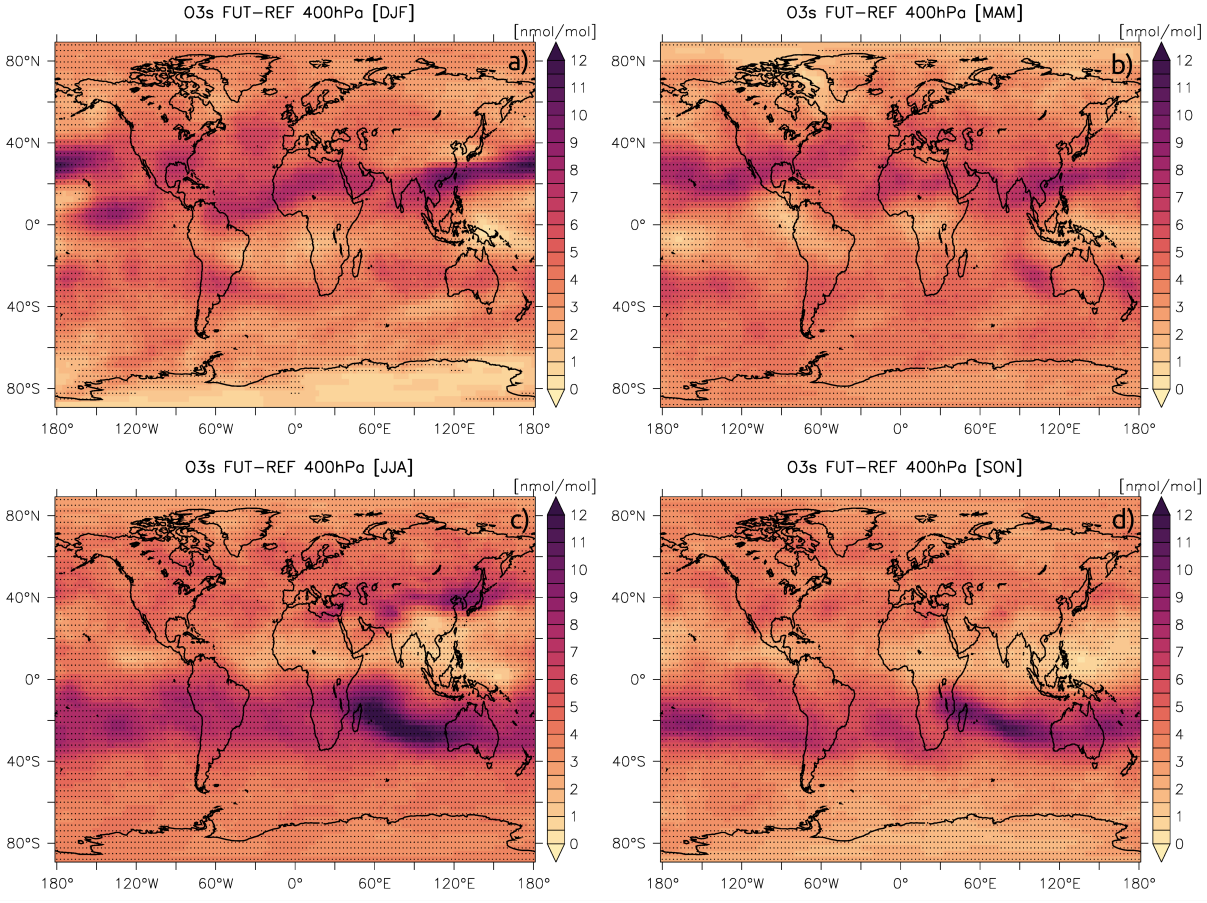

Figure 7. Mean stratospheric ozone tracer (O3s) concnentrations differences (shaded; $\mathrm{nmol/mol}$) between the FUT and REF periods at 400 hPa for DJF (a), MAM (b), JJA (c) and SON (d). Black dots denote statistically significant differences at the 99% significance level.

https://doi.org/10.5194/acp-2019-508
Preprint. Discussion started: 14 June 2019

Atmospheric Chemistry and Physics Discussions

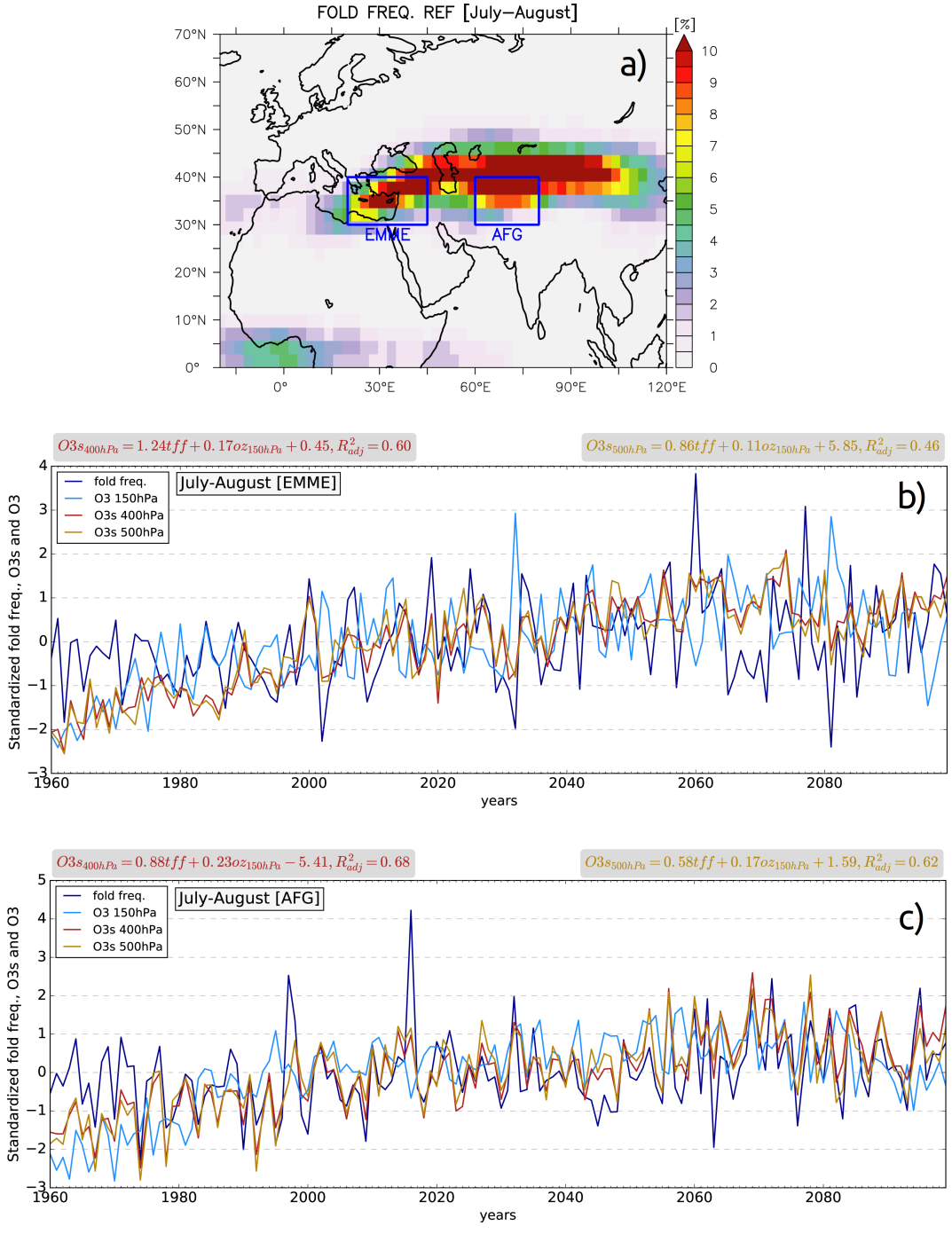

Figure 8. Mean July-August tropopause fold frequency (%) during the REF period and the examined EMME (20-45°E,30-40°N) and AFG (60-80°E, 30-40°N) regions (a). Timeseries of mean July-August tropopause folds frequency (dark blue line), O3 at 150 hPa (light blue line), O3s at 400 hPa (dark red line) and O3s at 500 hPa (orange line) over EM (b) and AFG (c) for the period 1960-2100. Regression equations for O3s at 400 and 500 hPa are also shown at the top of the charts with dark red and orange colours respectively.